Spectrochimica Acta Part A: Molecular and Biomolecular Spectroscopy 97 (2012) 388–396

Contents lists available at SciVerse ScienceDirect

Spectrochimica Acta Part A: Molecular and Biomolecular Spectroscopy

journal homepage: www.elsevier.com/locate/saa

Synthesis, spectroscopic, photoluminescence properties and biological evaluation of novel Zn(II) and Al(III) complexes of NOON tetradentate Schiff bases

Ayman A. Abdel Aziz, Ibrahim H.A. Badr *[,1], Ibrahim S.A. El-Sayed

Department of Chemistry, Faculty of Science, Ain Shams University, 11566 Cairo, Egypt

HIGHLIGHTS

- Novel Zn(II) and Al(III) salen complexes were synthesized and fully characterized.
- The complexes exhibited intense fluorescence at room temperature.
- The complexes are promising candidates as photoactive materials and anion carriers.
- The novel complexes exhibited remarkable antimicrobial activities.

GRAPHICAL ABSTRACT

Synthetic route of Zn(II) and Al(III) with tetradentate Schiff bases H_2L^{1-2}.

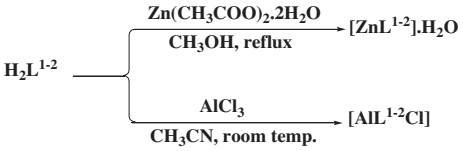

ARTICLE INFO

Article history:
Received 9 April 2012
Received in revised form 2 June 2012
Accepted 10 June 2012
Available online 28 June 2012

Keywords:
NOON Schiff bases
Zn(II) and Al(III) complexes
Characterization
Photoluminescence
Microbial activities

ABSTRACT

Novel mononuclear Zn(II) and Al(III) complexes were synthesized from the reactions of $Zn(OAc)_2{\cdot}2H_2O$ and anhydrous $AlCl_3$ with neutral N2O2 donor tetradentate Schiff bases; N,N′bis(salicylaldehyde)4,5-dimethyl-1,2-phenylenediamine (H_2L^1) and N,N′bis(salicylaldehyde)4,5-dichloro-1,2-phenylenediamine (H_2L^2). The new complexes were fully characterized by using micro analyses (CHN), FT-IR, ^{1}H NMR, UV–Vis spectra and thermal analysis. The analytical data have been showed that, the stoichiometry of the complexes is 1:1. Spectroscopic data suggested tetrahedral and square pyramidal geometries for Zn(II) and Al(III) complexes, respectively. The synthesized Zn(II), and Al(III) complexes exhibited intense fluorescence emission in the visible region upon UV-excitation in methylene chloride solution at ambient temperature. This high fluorescence emission was assigned to the strong coordination of the ligands to the small and the highly charged Zn(II) and Al(III) ions. Such strong coordination seems to extend the π-conjugation of the complexes. Thermal analysis measurements indicated that the complexes have good thermal stability. As a potential application the biological activity (e.g., antimicrobial action) of the prepared ligands and complexes was assessed by in-vitro testing of their effect on the growth of various strains of bacteria and fungi.

Introduction

Schiff-base ligands have received more and more attention, mainly because of their wide application in the fields of synthesis [1], catalysis [2,3], solid phase extraction of metal ions [4], various types of polymerization [5], biological application as antibacterial, antifungal, anti-inflammatory herbicidal properties and antitumor agents [6,7]. Furthermore, Schiff bases and other macrocyclic ligands as well as their complexes are widely used for the preparation of highly selective polymer membrane electrodes [8–12], optical sensors and biological probes [13–15]. This attention is still growing and considerable research effort is still devoted to the synthesis of new Schiff-base complexes with transition [16,17] and main group metal ions [18–20].

At present, much attention has been paid to complexes of Zn(II) and Al(III) Schiff base ligands, exhibiting luminescent properties

* Corresponding author. Present address: Taibah University, Faculty of Applied Science, Department of Applied Chemistry, Al Madinah, Saudi Arabia. Tel.: +966 0500213248; fax: +966 048494531.
E-mail address: ibadr1@yahoo.com (I.H.A. Badr).
[1] Chemistry Department, Faculty of Science, Ain Shams University, Cairo, Egypt.

1386-1425/$ - see front matter © 2012 Elsevier B.V. All rights reserved.
http://dx.doi.org/10.1016/j.saa.2012.06.023

[21–27]. Such complexes are promising materials for optoelectronic applications due to their outstanding photo and electroluminescent (PL and EL) properties [28,29].

Herein, we report the synthesis, spectroscopic characterization, photophysical properties and thermal analysis of novel Zn(II) and Al(III) complexes with salen derivatives N,N′bis(salicylaldehyde)4,5-dimethyl-1,2-phenylenediamine (H_2L^1), and N,N′bis(salicylaldehyde)4,5-dichloro-1,2-phenylenediamine (H_2L^2),(Scheme 1). Fluorescence emission upon complex formation opens up the opportunity for photochemical applications of these complexes. Furthermore, the bio-efficacy of ligands and the synthesized complexes were tested in-vitro against various strains of bacteria and fungi at different concentration levels to evaluate their utility as potential antimicrobial agents.

Experimental

Materials

4,5-Dimethyl-1,2-phenylendiammine, 4,5-dichloro-1,2-phenylendiammine, salicylaldehyde, $Zn(CH_3COO)_2{\cdot}2H_2O$ and $AlCl_3$ were supplied from Aldrich. All solvents were of analytical grade.

Instrumentation

Carbon, hydrogen and nitrogen were determined using JEOL JMS-AX500 elemental analyzer. Infrared spectra (4000–400 cm^{-1}) were recorded with KBr optics on a Unicam-Mattson 1000 FT-IR. ^1H NMR measurements were performed on a Spectrospin-Bruker AC 200 MHz spectrometer using DMSO-d_6 as a solvent and TMS as an internal reference. All conductivity measurements were performed in DMSO (1×10^{-3} M) at 25 °C, by using Jenway 4010 conductivity meter. The thermal behavior was monitored by a Shimadzu DT-50 thermal analyzer under nitrogen atmosphere with a heating rate of 10 °C/min. UV–Vis spectra were recorded using a Shimadzu UV 1800 Spectrophotometer. The UV spectrometer is controlled with a PC by using UVProbe software, version 2.34. The photoluminescence properties of all compounds were studied using a Jenway 6270 Fluorimeter. All samples were prepared in spectroscopic grade methylene chloride (1×10^{-5} M) and analyzed in a 1 cm optical path quartz cuvette. The photoluminescence quantum efficiencies of the complexes were calculated by using quinine sulfate as reference quantum yield standard (λ_{ex} = 410 nm, quantum yield = 0.54 in 0.1 mol L^{-1} H_2SO_4) [30,31].

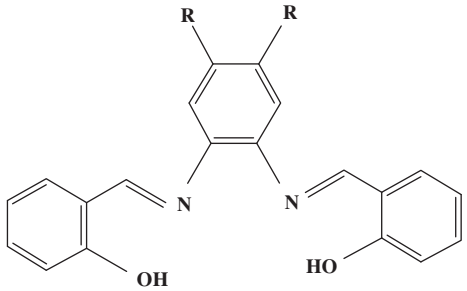

R = CH_3 H_2L^1

R = Cl H_2L^2

Scheme 1. Chemical formula of the tetradentate Schiff bases H_2L^{1-2}.

Syntheses

Microwave assisted solvent-free synthesis of the Schiff base ligand (H_2L^{1-2})

The ligands H_2L^{1-2} were synthesized as described in literature [32]. To enhance the yield and reduce the time a microwave synthesis method was used. 0.1 mol of the diamine derivative and 0.2 mol of salicylaldehyde were mixed well in a 50 ml Pyrex beaker and the mixture was irradiated in a microwave oven for one minute. The yellow product obtained was separated, dried and recrystallized from ethanol. The purity of the ligand was checked by TLC.

Synthesis of Zn(II) complexes

$Zn(OAc)_2{\cdot}2H_2O$ (1.0 mmol) was dissolved in methanol (10 mL) and heated using a water bath to ensure complete dissolution of the salt, then added gradually to a hot stirred solution of the ligand (1.0 mmol) dissolved in methanol (10 mL). The mixture was further heated on a hot plate at 60 °C for 2 h to ensure complete precipitation of the yellow complexes. The precipitated solid was filtered, washed with cold methanol and hot petroleum ether 40–60 °C, recrystallized from ethanol and finally dried under vacuum. The purity of the complexes was checked by TLC.

Synthesis of Al(III) complexes

Al(III) complexes were obtained from appropriate ligands upon the reaction with anhydrous $AlCl_3$ in dry acetonitrile at room temperature. This procedure was successfully applied in earlier work [11]. $AlCl_3$ (0.200 g, 1.5 mmol) was added to a solution of 1 mmol of free ligands in 20 mL of freshly distilled acetonitrile. A yellow precipitate was formed immediately. The precipitated product was filtered off, washed with cold ethyl acetate and dried under vacuum. The complex was purified by crystallization from ethyl acetate/ethanol mixture.

Scheme 2 represents the synthetic route of synthesis of Zn(II) and Al(III) complexes.

Determination of the metal content of the complexes

An accurately weighed portion of the solid complex under investigation in the range from 10 to 30 mg was placed in Kjeldahl flask. Concentrated nitric acid (5–10 mL) was added to start the fast wet oxidation digestion. This mixture was digested by a gradual heating with a concomitant dropping of H_2O_2 solution. This treatment was conducted until the entire solid complex was dissolved. The obtained clear solution was diluted up to exactly 50 mL by de-ionized water and the metal content was determined by standard analytical methods described in literature [33].

Determination of fluorescence quantum yield of Zn(II) and Al(III) complexes

Determination of the relative quantum yield is generally accomplished by a comparison of the wavelength-integrated emission intensity of the unknown sample with that of a reference material. The fluorescence quantum yields of Zn(II) and Al(III) complexes were determined using quinine sulfate as a reference with a known Φ_R of 0.546 as measured in 0.5 M sulfuric acid [34]. The

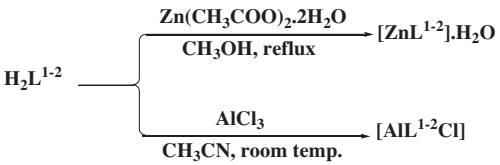

Scheme 2. Synthetic route of Zn(II) and Al(III) with tetradentate Schiff bases H_2L^{1-2}.

Table 1
Elemental analyses and some physical properties of the Schiff base ligands (H_2L^{1-2}) and their complexes.

Compounds	Yield (%)	M.Wt	Color	(Calculated) Found (%)					Λ_m (Ω^{-1} cm^2 mol^{-1})
				C	H	N	Cl	**M**	
H_2L^1 ($C_{22}H_{20}N_2O_2$)	63	344.41	Yellow	(76.72) 76.21	(5.85) 5.72	(8.13) 7.98	–	–	–
H_2L^2 ($C_{20}H_{14}N_2O_2Cl_2$)	70	385.25	Yellow	(62.35) 62.19	(3.66) 3.60	(7. 27) 7.25	(18.40) 18.38	–	–
[$C_{22}H_{18}N_2O_2Zn$]·H_2O (1)	95	425.80	Yellow	(62.05) 61.98	(4.26) 4.79	(6.57) 6.13	-	(15.35) 15.27	13.43
[$C_{20}H_{12}N_2O_2Cl_2Zn$]·H_2O (2)	87	466.64	Yellow	(51.47) 50.98	(2.59) 2.48	(6.00) 5.86	(15.19) 15.01	(14.01) 13.97	12.47
[$C_{22}H_{18}N_2O_2ClAl$] (3)	79	404.83	Yellow	(65.27) 61.09	(4.48) 4.32	(6.91) 6.53	(8.75) 8.09	(6.66) 6.24	9.49
[$C_{20}H_{12}N_2O_2Cl_3Al$] (4)	81	445.66	Yellow	(53.90) 53.16	(2.71) 2.51	(6.28) 6.17	(23.86) 23.72	(6.05) 5.99	10.95

Table 2
The infrared (cm^{-1}, KBr) data of the Schiff base ligands and their complexes.

Compound	ν (OH)	ν (C=N)	ν (C–O)	ν (M–N)	ν (M–O)
H_2L^1	3428(m, br)	1617(s)	1278(m)	–	–
H_2L^2	3444(m, br)	1616(s)	1279(m)	–	–
[ZnL^1]·(H_2O) (1)	3415(m, br)	1619(s)	1321(m)	443(w)	466(w)
[ZnL^2]·(H_2O) (2)	3411(m, br)	1614(s)	1322(m)	462(w)	499(w)
[AlL^1Cl] (3)	–	1621(s)	1283(m)	424(w)	448(w)
[AlL^2Cl] (4)	–	1618(s)	1304(m)	479(w)	591(w)

* br, broad; s, strong; m, medium; w, weak.

area of the emission spectrum was integrated and the quantum yield was calculated according to the following equation [35]:

$$\frac{\Phi_S}{\Phi_R} = \left[\frac{A_S}{A_R}\right]\left[\frac{(OD)_R}{(OD)_S}\right] \times \left[\frac{\eta_S^2}{\eta_R^2}\right]$$

where Φ_S and Φ_R are the fluorescence quantum yields of the sample and reference, respectively, A_S and A_R are the areas under the fluorescence emission peak of the sample and that of the reference, respectively. $(OD)_S$ and $(OD)_R$ are the respective optical densities of the sample and the reference solution at the wavelength of excitation. η_S and η_R are the values of refractive indices of the solvent used for the sample and that of the reference, respectively.

Antimicrobial screening

The antimicrobial activity of the synthesized compounds was tested against various micro-organisms. The in-vitro growth inhibitory of the ligands and their complexes were performed against different types of bacteria; *Staphylococcus aureus*, *Staphylococcus epidermidis*, *Bacillus megaterium*, *Escherichia coli*, *Pseudomonas aeruginosa* and *Klebsiella pneumoniae* in Mueller Hinton-Agar medium. The antifungal activity was tested against the fungi; *Aspergillus niger*, *Aspergillus flavus*, *Curvularia lunata*, *Rhizoctonia bataticola*, *Candida albicans*, and *Fusarium solani*, cultured on YPD-agar medium. Preliminary screening was performed using two concentrations, 125 μg/1.0 mL and 250 μg/1.0 mL of the tested compounds dissolved in DMSO. The in-vitro antimicrobial activity of the free ligands and their complexes were tested using the general procedure described in the literature [36,37] as follows: 0.5 mL spore suspension (106–107 spore mL^{-1}) of each of the investigated organisms was added to a sterile agar medium just before solidification, then poured into sterile Petri dishes (9 cm in diameter), and left to solidify. Using a sterile cork borer (6 mm in diameter), wells were made in each dish, then 0.1 mL of the tested compounds dissolved in DMSO were poured into three wells and the dishes were incubated at 37 ± 0.1 °C for 48 h (in case of bacteria) and 30 ± 0.1 °C for 72 h (in case of fungi). The growth of the microorganisms was inhibited by diffusion of the test solutions and then the inhibition zones around each well were measured. The effectiveness of an antimicrobial agent is based on the size of the inhibition zones. The diameter of the zone is measured to the nearest millimeter (mm). The antibacterial activity of each compound was compared with that of standard antibiotics such as Streptomycin, Chloramphenicol and Amoxycillin. The antifungal activity of the test compound was compared with Nystatin, Tetracycline and Chlorometazole as standard antifungal. DMSO was used as a control under the same conditions for each organism and no activity was found. The activity results were calculated as a mean of triplicates.

Results and discussion

Novel mononuclear Zn(II) and Al(III) complexes have been synthesized from the reactions of $Zn(OAc)_2{\cdot}2H_2O$ and anhydrous $AlCl_3$ with neutral [N2O2] donor tetradentate Schiff bases namely: N,N′bis(salicylaldehyde)4,5-dimethyl-1,2-phenylenediamine (H_2L^1), N,N′bis(salicylaldehyde)4,5-dichloro-1,2-phenylenediamine (H_2L^2). The prepared complexes have been characterized by several techniques using elemental analyses (CHN), FT-IR, ^{1}H NMR, UV–Vis spectra and thermal studies. All the metal complexes have yellow color, stable in air, insoluble in water and soluble in $CHCl_3$, CH_2Cl_2 and DMSO. The analytical data obtained suggested 1:1 (M:L) stoichiometry for the complexes. The molar conductivity (Λ_m) of 1×10^{-3} M solutions of the complexes in DMSO at 25 °C fall in the range 9.49–13.43 Ω^{-1} cm^2 mol^{-1}, indicating non-electrolytic nature of the complexes [38]. Elemental analyses and some physical properties of the ligands and their complexes are listed in Table 1.

Characterization of N2O2 ligands and their complexes

FT-IR spectra

The FT-IR spectra of the two N2O2 ligands and complexes are summarized in Table 2. Fig. S1(a) and (b) are given as

Table 3
The ^{1}H NMR spectral data (δ, ppm) of the Schiff bases ligands and their complexes.

Compound	OH(phenolic)	CH=N	Aromatic protons	Aliphatic protons (–CH_3)
H_2L^1	13.12(s)	8.96(s)	6.95–7.69(m)	2.33(s)
H_2L^2	12.57(s)	9.01(s)	6.98–7.85(m)	
[$Zn(L^1)$]·H_2O (1)	–	9.03(s)	6.47–7.70(m)	2.31(s)
[$Zn(L^2)$]·H_2O (2)	–	9.07(s)	6.49–7.48(m)	
[$Al(L^1)Cl$] (3)	–	9.26(s)	6.83–7.79(m)	2.30(s)
[$Al(L^2)Cl$] (4)	–	9.37(s)	6.86–7.69(m)	

s, singlet; m, multiplet.

Table 4
Absorption and photoluminescent for solutions of Schiff bases ligands and their complexes.

Compound	UV–Vis λ_{max}(nm)		λ_{ex}	λ_{em}	Stoke shift ($\Delta\lambda$)	Quantum yield Φ_f
	π–π^*	n–π^*				
H_2L^1	232	328	328	408	80	0.06
H_2L^2	212	288	288	404	116	0.01
$[Zn(L^1)]\cdot H_2O$ (1)	244	364	364	494	130	0.35
$[Zn(L^2)]\cdot H_2O$ (2)	234	332	332	482	150	0.21
$[Al(L^1)Cl]$ (3)	238	340	340	476	136	0.26
$[Al(L^2)Cl]$ (4)	218	320	320	460	140	0.15

* All measurements were carried out at room temperature in 1×10^{-5} M CH_2Cl_2 solution.

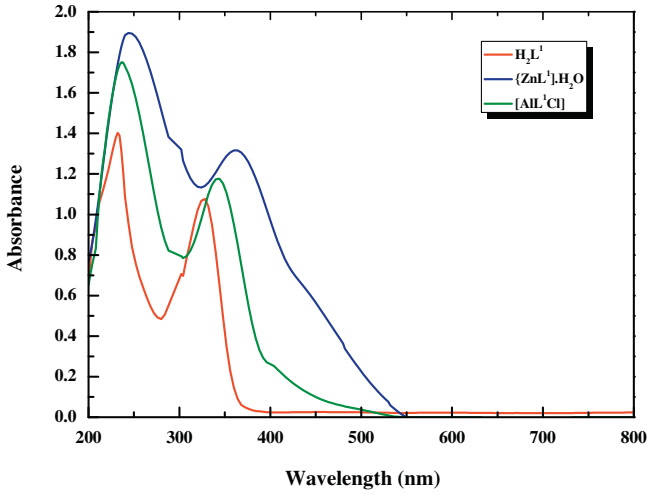

Fig. 1. UV–Vis spectra of H_2L^1, $[ZnL^1]\cdot H_2O$ and $[AlL^1Cl]$ in methylene chloride (1×10^{-5} M).

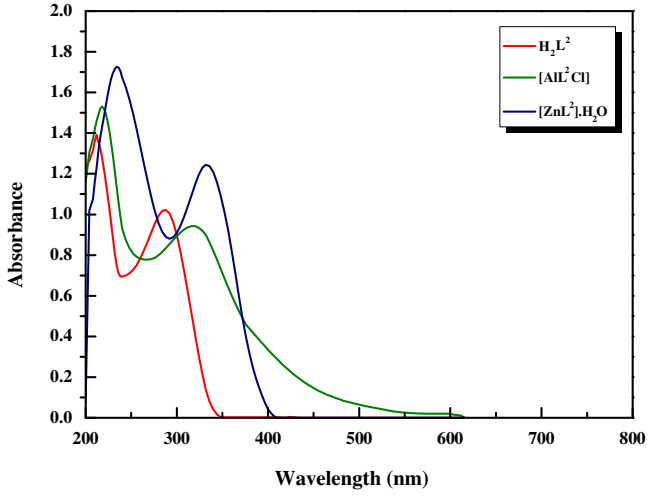

Fig. 2. UV–Vis spectra of (H_2L^2), $[ZnL^2]\cdot H_2O$ and $[AlL^2Cl]$ in methylene chloride (1×10^{-5} M).

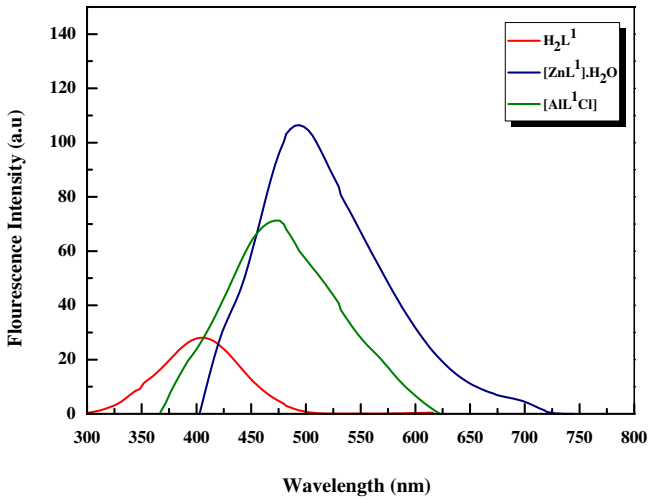

Fig. 3. Fluorescence spectra of H_2L^1, $[ZnL^1]\cdot H_2O$ and $[AlL^1Cl]$ in methylene in methylene chloride (1×10^{-5} M).

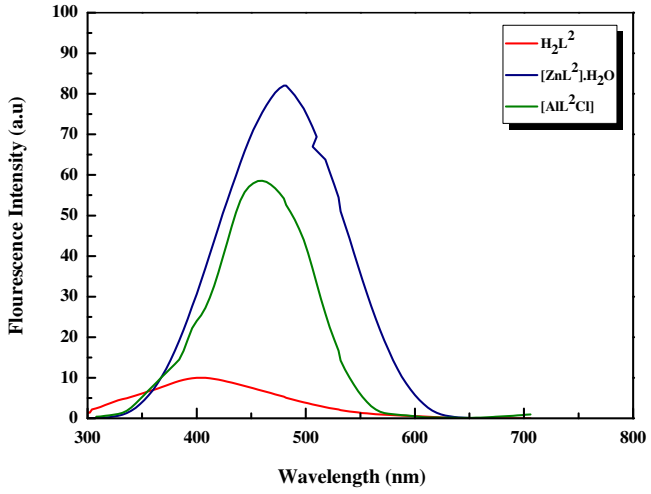

Fig. 4. Fluorescence spectra of H_2L^2, $[ZnL_2]\cdot H_2O$ and $[AlL^2Cl]$ in methylene chloride (1×10^{-5} M).

representative examples of the FT-IR spectra of Zn(II) and Al(III) complex of H_2L^2. The FT-IR spectra of the complexes are compared with those of the free ligands in order to determine the coordination sites which are involved in chelation. The position and/or the intensities of the peaks of the chelation sites are expected to change upon coordination. New peaks are also guiding peaks as well as peaks of water of chelation. The discussion is confined to the most important vibrations of the 4000–400 cm^{-1} region in relation to structure. It was clearly seen that the absence of the characteristic aldehydic carbonyl stretching bands, and the appearance of the azomethine –C=N– bands, at 1617 cm^{-1} and 1616 cm^{-1} for H_2L^1 and H_2L^2, respectively, indicating the formation of the Schiff bases. The broad band of medium intensity in the region 3428–3444 cm^{-1} was attributed to the intra-molecular hydrogen-bonded O–H group [39]. The broadness of this band was attributed to the internal hydrogen bond OH···N=C [40]. As the hydrogen bond becomes stronger, the bandwidth increases, and this band sometimes cannot be detected [41]. This band was

Table 5
Thermogravimetric characteristics of Zn(II) and Al(III) complexes.

Complex	Temp. range (°C)	Mass loss (%) (calc.) found	Assignment	Residue
$[C_{22}H_{18}N_2O_2Zn]\cdot H_2O$ (1)	187–245	(4.23) 4.19	H_2O	ZnO
	373–683	(76.65) 76.54	$C_{22}H_{18}N_2O$	
$[C_{20}H_{12}N_2O_2Cl_2Zn]\cdot H_2O$ (2)	182–250	(3.86) 3.67	H_2O	ZnO
	326–508	(78.69) 78.47	$C_{20}H_{12}N_2OCl_2$	
$[C_{22}H_{18}N_2O_2ClAl]$ (3)	218–268	(8.75) 8.65	$½Cl_2$	Al
	400–513	(25.72) 25.69	C_8H_8	
	591–768	(58.85) 58.67	$2C_7H_5NO$	
$[C_{20}H_{12}N_2O_2Cl_3Al]$ (4)	219–243	(7.95) 7.83	$½Cl_2$	Al
	368–454	(32.53) 32.39	$C_6H_2Cl_2$	
	500–683	(53.45) 53.37	$2C_7H_5NO$	

missing in the spectra of Al(III) complexes due to deprotonation upon complexation. On the other hand, the FT-IR spectra of Zn(II) complexes exhibited a broad band at 3411–3415 cm^{-1} which renders it difficult to be attributed to the involvement of phenolic-OH group in coordination. However the deprotonation of phenolic –OH groups of the ligands upon complexation with Zn(II) was approved by the disappearance of the signal of the –OH group in the ^1H NMR spectra of Zn(II) complexes as it will be discussed later. Coordination of the Schiff base to the metal through the nitrogen atom is expected to reduce electron density in the azomethine as a result of the withdrawal of electron density from the nitrogen atom and should lower the C=N absorption frequency [40]. Surprisingly, the FT-IR spectra of the complexes indicated that chelation of N2O2 ligands to Al(III) and Zn(II) strengthened the C=N bonds except for $[ZnL^2]\cdot H_2O$ (see data in Table 2). This could be due to the effect of different substituents in the diamine bridge, which may alter conjugation of the ligands. Although the change in the FTIR peak of C=N does not support the involvement of this group in chelation, other FTIR peaks and the ^1H NMR spectra strongly support the chelation of this group to the metal ion center (see discussion below).

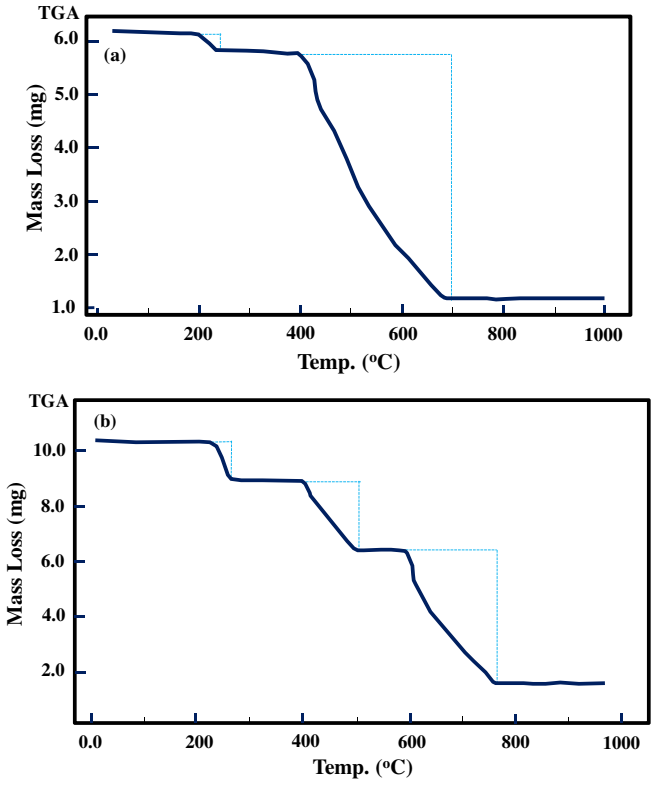

Fig. 5. TGA curve of: (a) $[ZnL^1]\cdot H_2O$ complex; (b) $[AlL^1Cl]$ complex.

Furthermore, the involvement of the deprotonated phenolic-OH group in chelation was confirmed by clarifying the effect of chelation on the ν(C–O). The medium intensity band in the region 1278–1279 cm^{-1} was ascribed to the phenolic C–O stretching vibration in the case of salicylideneanilines [42]. On complexation this band was shifted to higher frequency in the range 1283–1322 cm^{-1} for complexes. The shift of (C–O) band to higher frequency suggested the strengthening of the (C–O) bond upon deprotonation of the o-OH group of Schiff base moiety [43]. Further evidences of the coordination of the azomethine nitrogen and phenolic oxygen were supported by the appearance of two non-ligand weak bands at 448–591 cm^{-1} and 424–479 cm^{-1} which were assigned to ν(M–O) and ν(M–N) [44], respectively. This supports that the bonding of the ligands to the metal ions was achieved by the phenolic oxygen atoms and the azomethine nitrogen atoms of the ligands. Therefore, the above arguments together with the elemental analyses indicated that, the Schiff bases ligands behaved as a dibasic tetradentate ligands coordinated to the metal ions with NOON donor sites of the azomethine –N and phenolate –O.

^1H NMR spectra

Further evidence of the bonding mode of the ligands was also provided by the ^1H NMR spectra of the Schiff base ligands and their diamagnetic Zn(II) and Al(III) complexes. The chemical shifts of different types of protons in the ^1H NMR spectra of the N2O2 ligands and their complexes are given in Table 3. ^1H NMR spectra of Zn(II) and Al(III) complexes with H_2L^1 is shown in Fig. S2 (a) and (b) as representative examples for the ^1H NMR data obtained for the prepared compounds. The ^1HNMR spectra of the parent ligands H_2L^{1-2} showed singlet signal at very downfield in the region δ 12.57–13.12 ppm, which was attributed to two phenolic -OH protons. The OH signals disappear with addition of the D_2O [45]. The ligands also showed singlet in the region δ 8.96–9.01 ppm which was attributed to the azomethine (–CH=N–) protons [46]. The ^1H NMR spectra of the ligands revealed multiplets in the range 6.95–7.85 ppm which was attributed to aromatic protons [47]. A sharp singlet appeared at δ 2.33 ppm in the spectra of H_2L^1 which was assigned to methyl protons attached to the benzene ring of the diamine. A comparison of ^1H NMR spectra of the free Schiff base ligands with that of the corresponding diamagnetic complexes of Zn(II) and Al(III) revealed that the chemical shifts observed for the OH protons of the ligands have disappeared in all complexes. The absence of –OH signals indicated deprotonation of the hydroxyl group of the Schiff bases and confirmed the bonding of oxygen to the metal ions (C–O–M) [48] and supports the FTIR findings. It is well-know that the ^1H NMR spectra can provide compelling evidence for the presence of either one or two azomethine groups. Indeed, the presence of only one sharp singlet for the –C(H)=N proton clearly indicated that the magnetic environment is equivalent for all such protons, suggesting the presence of a planar ligand in these complexes [49]. In case of Zn(II) and Al(III) complexes, the position of azomethine signal was shifted to downfield region

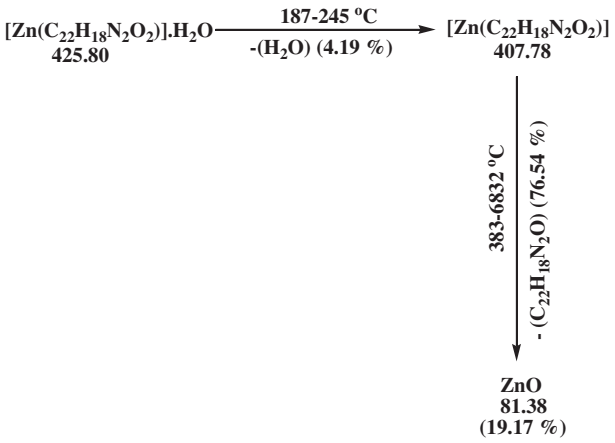

Scheme 3. Thermal decomposition steps of $[ZnL^1]\cdot H_2O$ complex.

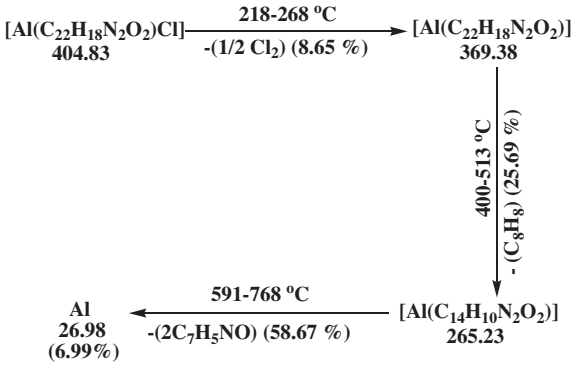

Scheme 4. Thermal decomposition steps of $[AlL^1Cl]$ complex.

9.03–9.37 ppm in comparison with that of the free ligands, inferring coordination through the azomethine nitrogen atom of the ligand [50]. This suggested deshielding of the azomethine proton and proved the coordination of the azomethine group to the central metal ion. The multiplets, assigned to the aromatic protons, were displaced upper field around the region δ 6.47–7.79 (Table 3). It can be also noticed that the proton signal of $-CH_3$ at 2.33 ppm (in case of the complexes of the ligand H_2L^1) was slightly affected by chelation.

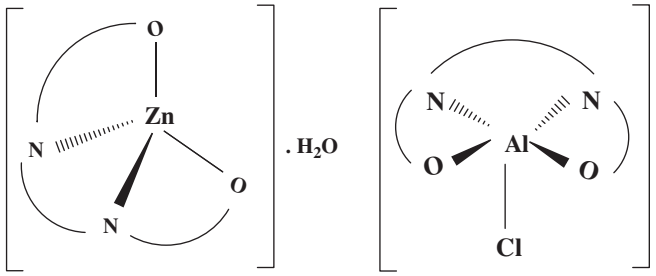

Scheme 5. The proposed structure of Zn(II) and Al(III) complexes.

Photophysical properties

The optical properties of the Schiff base ligands and their complexes were explored in methylene chloride solution (1×10^{-5} M) using UV–Vis and photoluminescence. Table 4 summarizes the absorption and emission data for the ligands and their complexes. The UV–Vis absorption spectra of the ligands and their complexes are shown in Figs. 1 and 2. As can be seen the absorption spectra of the Schiff base ligands exhibited two high intensity bands around 212–232 nm and 288–328 nm, designated as π–π^* and n–π^* transitions, respectively, for the electrons localized on the C=N chromophore. The absorption spectra of Zn(II) and Al(III) complexes have similar pattern to that of the free ligands yet their spectra indicated a bathochromic shift, which confirms the formation of Schiff base metal complexes. As expected for the diamagnetic Zn(II) (d^{10}) and Al(III) (d^0) configuration, ligand field band due to d–d electronic transitions is not expected [51] and the trends observed for the ligands were maintained after coordination.

The study of photoluminescence (PL) of Zn(II) and Al(III) complexes is not only of fundamental interest, but also significant for different applications (optical amplifiers, optical waveguides, OLED, etc.) [52]. In this work steady-state fluorescence studies have been employed as an independent evidence of complexation between the ligands and the metal ions. Figs. 3 and 4 represent the luminescence spectra of the ligands and their corresponding complexes. Photoluminescence studies were carried out at room temperature in methylene chloride solution. The emission spectra were obtained by excitation at the longest wavelength of the absorption peaks. All the prepared Schiff bases, and their Zn(II), Al(III) complexes emit in the visible region of spectrum upon the UV excitation. The photoluminescence spectra of the Zn(II) and Al(III) complexes were assigned to energy transfer between the HOMO and LUMO of the deprotonated ligands with the HOMO mainly being π-bonding in character and the LUMO mainly being π^* antibonding in character. To sum up, the luminescence has been caused by the $\pi \rightarrow \pi^*$ transition between the ligand orbitals (ligand

Table 6
Antibacterial activity of the Schiff base ligands (H_2L^{1-2}) and their complexes.

Compound	Antibacterial activity of zone of inhibition, mm											
	S. aureus		*S. epidermidis*		*B. megaterium*		*E. coli*		*P. aeruginosa*		*K. pneumoniae*	
	A	B	A	B	A	B	A	B	A	B	A	B
H_2L^1	7	8	6	9	7	10	8	10	6	10	8	11
H_2L^2	8	11	16	18	12	16	10	13	10	12	14	17
$[Zn(L^1)]\cdot H_2O$ (1)	17	21	13	21	13	18	12	17	11	17	10	16
$[Zn(L^2)]\cdot H_2O$ (2)	21	26	17	24	15	21	14	20	14	20	18	21
$[Al(L^1)Cl]$ (3)	12	17	10	15	11	16	11	16	11	16	16	21
$[Al(L^2)Cl]$ (4)	16	19	12	17	12	15	12	16	12	18	16	20
Streptomycin	24	28	19	27	20	26	21	24	20	24	17	26
Chloramphenicol	23	29	21	29	22	28	21	29	22	27	20	29
Amoxycillin	22	27	20	24	19	24	18	22	18	23	19	25
DMSO	0	0	0	0	0	0	0	0	0	0	0	0

A, 125 μg/1.0 mL; B, 250 μg/1.0 mL.

Table 7
Antifungal activity of the Schiff base ligands (H_2L^{1-2}) and their complexes.

Compound	Antifungal activity of zone of inhibition, mm											
	A. niger		*A. flavus*		*C. lunata*		*R. bataticola*		*C. albicans*		*F. solani*	
	A	B	A	B	A	B	A	B	A	B	A	B
H_2L^1	12	14	10	13	9	11	9	11	10	14	8	11
H_2L^2	12	13	14	16	12	16	11	13	15	18	13	15
$[Zn(L^1)]\cdot H_2O$ (1)	13	17	16	20	18	23	15	20	18	21	16	19
$[Zn(L^2)]\cdot H_2O$ (2)	15	20	18	22	20	27	18	23	19	25	19	24
$[Al(L^1)Cl]$ (3)	13	16	12	17	11	13	11	13	13	18	11	14
$[Al(L^2)Cl]$ (4)	14	18	15	19	13	19	11	15	12	17	11	16
Nystatin	17	21	17	21	19	22	18	22	18	22	17	21
Tetracycline	21	28	18	23	22	29	19	24	17	21	19	25
Chlorometazole	24	29	23	27	23	28	22	27	24	28	22	26
DMSO	0	0	0	0	0	0	0	0	0	0	0	0

A, 125 μg/1.0 mL; B, 250 μg/1.0 mL

to ligand charge transfer) [53]. The enhancement of the fluorescence of the complexes compared to their respective ligands is due to CHEF (chelation enhancement of fluorescence emission) [54]. Factors like a simple binding of the ligand to the metal ions [55], an increase in rigidity of structure [56], a restriction in the photo induced electron transfer (PFT) [54,57] etc. are assigned to the appearance and enhancement of the PL. In the present case, the first two factors seem to be responsible for the enhancement PL.

The position of emission maximum and the quantum yield of luminescence depend on the structure of the complexes and their ligands. The observed differences in the PL properties of the prepared compounds may be caused by structural variations in the conjugation systems. The effect of the substituents in the diamine bridge has been also studied. Indeed, complexes with Schiff bases bearing electrondonating substituents ($-CH_3$) are shifted in the bathochromic direction compared to those with electronwithdrawing substituents (–Cl). It is plausible that the $-CH_3$ group in H_2L^1 tends to activate the benzene ring and thus increases the freedom of the π-electrons. On the other hand –Cl group in H_2L^2 deactivates the ring by withdrawing the π-electrons from the ring thus reducing their freedom by increasing their localization [58]. Literature data showed that both conjugation enhancement and the introduction of electrondonating substituents should lead to a considerable decrease in the energy difference between the HOMO and LUMO [59,60].

Thermogravimetric analysis studies

The thermal studies of the reported complexes provided further insight into the proposed structures. The reported complexes were found to be air stable and have high thermal stability. The thermal stability is an important feature of a compound that could be utilized as EL material [61]. The thermal behavior of the complexes under investigation was assessed using thermogravimetric analysis (TGA). The samples were analyzed in a platinum pan under N_2 and the temperature was linearly increased at 10 °C min^{-1} over a temperature range 20–1000 °C.

The TG data for the synthesized complexes are summarized in Table 5 and TG plots of $[Zn(L^1)]\cdot H_2O$ and $[AlL^1Cl]$ complexes, as representative example, are shown in Fig. 5. As can be seen the TG plot of $[Zn(L^1)]\cdot H_2O$ complex (1) displayed two resolved and well-defined decomposition steps (Scheme 3). The first decomposition occurred in the temperature range 187–245 °C with a net weight loss of 4.20% (Calc. 4.23%) which is consistent with the elimination of H_2O molecule. The second decomposition step occurred in the temperature range 373–683 °C with a net weight loss of 76.54% (Calc. 76.65%). This decomposition step could be assigned to the elimination of $C_{22}H_{18}N_2O$ organic moiety to give finally ZnO residue with a net weight of 19.15% (Calc. 19.11%). The TGA plot $[ZnL^2]\cdot H_2O$ complex (2) exhibited a similar pattern but the first decomposition step occurred in the range 182–250 °C and the second step occurred in the range 326–508 °C.

On the other hand the TG plots $[AlL^1Cl]$ and $[AlL^2Cl]$ complexes displayed a similar decomposition pattern with three resolved decomposition steps (see data in Table 5 and Fig. 5). The first decomposition is consistent with evolution of ½ Cl_2, whereas the second and third steps involved removal of organic ligand moiety, leaving Al as a final residue as presented in Scheme 4.

Thermal studies have shown that the stability of the prepared complex is in the following the order: $[ZnL^1]H_2O$ > $[ZnL^2]\cdot H_2O$ > $[AlL^1Cl]$ > $[AlL^2Cl]$. This order could be explained based on the fact that electron withdrawing group (–Cl) of the ligand reduces the stability of the complexes, while the electron donating group ($-CH_3$) increases the stability of the complexes [50].

Although different strategies were followed to prepare single crystals of the prepared compounds, we were unable to prepare single crystals for X-ray studies. Tetrahedral and square pyramidal geometry are proposed for the Zn(II) and Al(III) complexes, respectively (Scheme 5). Such geometries are suggested based on the interpretation of analytical, conductance, infrared and ^1H NMR spectral data.

Biological activity

The Schiff base ligands H_2L^{1-2} and their complexes (1–4) were tested for their inhibitory effects on the growth of different bacteria types: *S. aureus*, *S. epidermidis*, *B. megaterium*, *E. coli*, *P. aeruginosa K. pneumoniae* and different fungi types: *A. niger*, *A. flavus*, *C. lunata*, *R. bataticola*, *C. albicans* and *F. solani*. Such organisms can achieve resistance to antibiotics through biochemical and morphological modification [62]. The antibacterial and antifungal activities obtained for the prepared compounds are listed in Tables 6 and 7, respectively. The results indicated that most of the tested complexes displayed more activity against the same microorganisms compared to the parent ligands under identical experimental conditions. The observed antibacterial and antifungal activities are presented graphically in Fig. 6(a) and (b). The increase in the activity of the complexes compared to that of the ligands could be explained on the basis of Overtone's concept [62] and Tweedy's Chelation theory [63]. According to Overtone's concept of cell permeability, the lipid membrane that surrounds the cell favors the passage of only lipid-soluble materials. This makes liposolubility is an important factor that controls the antifungal activity. On chelation, the polarity of cation will be reduced to a greater extent due to the overlap of the ligand orbital. Further, the chelation increases

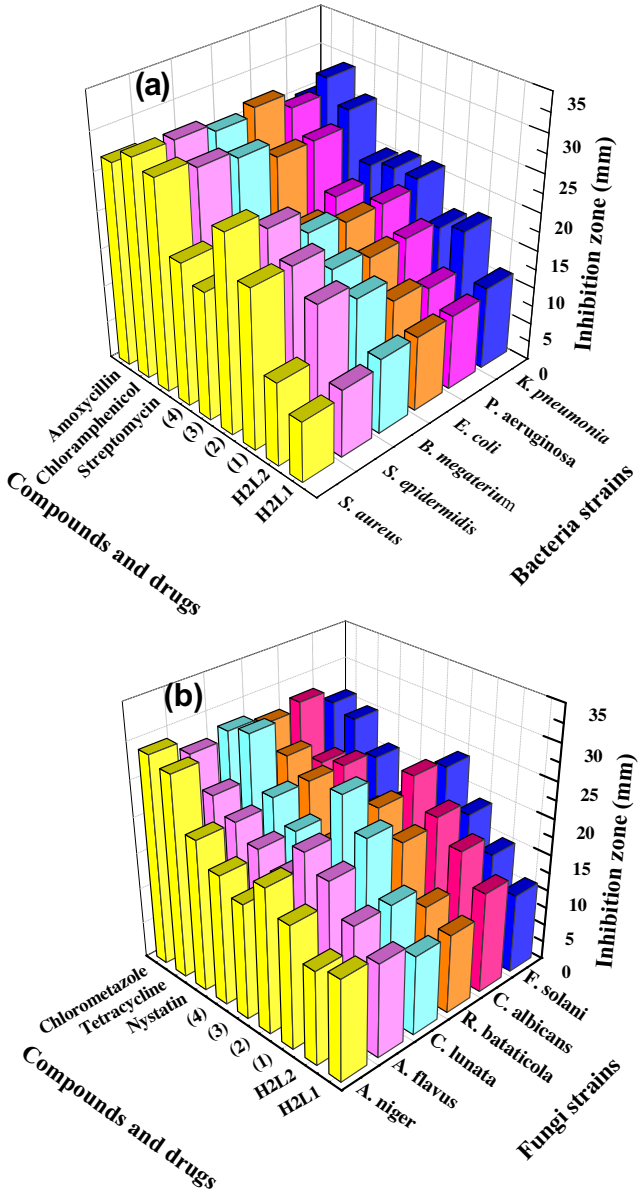

Fig. 6. Zone of inhibitions of reported compounds (250 μg/1.0 mL) and antibiotics against different bacteria strains (a) and different fungi strains (b).

the delocalization of π-electrons over the whole chelate ring and enhances the lipophilicity of the complexes. This increase in the lipophilicity enhances the penetration of the complexes into lipid membranes, and blocks the metal binding sites of the enzymes of the microorganism. Metal complexes also disturb the respiration process of the cell and thus block the synthesis of proteins which restricts further growth of the organism [63].

Generally, the electronic nature and position of substituents of the phenyl ring dictates the antimicrobial activities. The inhibitory action gets enhanced with the introduction of electronwithdrawing chloro groups in the phenyl ring, whereas electrondonating substituents such as methyl groups are less active compared to un-substituted phenyl ring [64].

Conclusions

Four mononuclear Zn(II) and Al(III) complexes were synthesized and fully characterized. The complexes were synthesized by the direct reaction between $Zn(OAc)_2{\cdot}2H_2O$ and anhydrous $AlCl_3$ with neutral N2O2 donor tetradentate Schiff bases namely: N,N′bis(salicylaldehyde)4,5-dimethyl-1,2-phenylenediamine (H_2L^1), and N,N′bis(salicylaldehyde)4,5-dichloro-1,2-phenylenediamine (H_2L^2). Spectral characterizations of the new complexes showed that Zn(II) forms four coordinate tetrahedral complexes with 1:1 (metal:ligand) stoichiometry. On the other hand, Al(III) forms five coordinate square pyramidal complexes. Thermal studies showed that the complexes have good thermal stabilities and follow the order: $[ZnL^1]H_2O$ > $[ZnL^2]{\cdot}H_2O$ > $[AlL^1Cl]$ > $[AlL^2Cl]$. Furthermore, the obtained research results indicated that Zn(II) complexes exhibit strong fluorescence at room temperature compared to Al(III) complexes. The PL behavior of Zn(II) and Al(III) complexes is particularly important for their potential application as photoactive materials. Interestingly the prepared complexes exhibited biological activity comparable to the well-known antibiotics.

Acknowledgements

The authors are grateful to the Scientific Research Sector of Ain Shams University (Grant 08-010) for providing financial support to undertake this work.

Appendix A. Supplementary data

Supplementary data associated with this article can be found, in the online version, at http://dx.doi.org/10.1016/j.saa.2012.06.023.

References

[1] D.A. Atwood, Coord. Chem. Rev. 165 (1997) 267–296.
[2] P.G. Cozz, Chem. Soc. Rev. 33 (2004) 410–421.
[3] A.A. Abdel Aziz, J. Mol. Struct. 979 (2010) 77–84.
[4] M. Shamsipur, A.R. Ghiasvand, H. Sharghi, H. Naeimi, Anal. Chim. Acta 408 (2000) 271–277.
[5] V.C. Gibson, R.K. O'Reilly, A.J.P. White, D.J. Williams, J. Am. Chem. Soc. 125 (2003) 8450–8451.
[6] S. Samadhiya, A. Halve, Orient. J. Chem. 17 (2001) 119–122.
[7] M.C. Rodrìguez-Argüelles, M.B. Ferrari, F. Bisceglie, C. Pelizzi, G. Pelosi, S. Pinelli, M. Sassi, J. Inorg. Biochem. 98 (2004) 313–321.
[8] I.H.A. Badr, Anal. Chim. Acta 570 (2006) 176–185.
[9] L.G. Bachas, M.F. Hawthorne, I.H.A. Badr, US patent 5985117, 1999.
[10] M.E. Meyerhoff, I.H.A. Badr, US patent 2006/0216194 A1, 2006.
[11] I.H.A. Badr, M. Diaz, M.F. Hawthorne, L.G. Bachas, Anal. Chem. 71 (1999) 1371–1377.
[12] A.A. Abdel Aziz, A.H. Kamel, Talanta 80 (2010) 1356–1363.
[13] I.H.A. Badr, M.E. Meyerhoff, Anal. Chim. Acta 553 (2005) 169–176.
[14] I.H.A. Badr, M.E. Meyerhoff, J. Am. Chem. Soc. 127 (2005) 5318–5319.
[15] I.H.A. Badr, M.E. Meyerhoff, Anal. Chem. 77 (2005) 6719–6728.
[16] A.A. Abdel Aziz, A.M. Salem, M.A. Sayed, M.M. Abouly, J. Mol. Struct. 1010 (2012) 130–138.
[17] H. Keypour, P. Arzhangi, N. Rahpeyma, M. Rezaeivala, Y. Elerman, O. Büyükgüngör, L. Valencia, H.R. Khavasi, J. Mol. Struct. 977 (2010) 6–11.
[18] D.A. Atwood, M.J. Harvey, Chem. Rev. 101 (2001) 37–52.
[19] J. Qiao, L.D. Wang, L. Duan, Y. Li, D.Q. Zhang, Y. Qiu, Inorg. Chem. 43 (2004) 5096–5102.
[20] A. Kagkelari, G.S. Papaefstathiou, C.P. Raptopoulou, T.F. Zafiropoulos, Polyhedron 28 (2009) 3279–3283.
[21] S. Aldridge, A.J. Downs, The Group 13 Metals Aluminium, Gallium, Indium and Thallium: Chemical Patterns And Peculiarities, first ed., John Wiley and Sons, Chichester, UK, 2011.
[22] M.S.J. Briggs, J.S. Fossey, C.J. Richards, B. Scott, J. Whately, Tetrahedron Lett. 43 (2002) 5169–5171.
[23] P.F. Wang, Z.R. Hong, Z.Y. Xie, S.W. Tong, O.Y. Wong, C.S. Lee, N.B. Wong, L.S. Hung, S.T. Lee, Chem. Commun. 2003 (2003) 1664–1665.
[24] M.L. Deda, M. Ghedini, I. Aiello, A. Grisolia, Chem. Lett. 33 (2004) 1060–1061.
[25] J. He, Y.G. Yin, X.C. Huang, D. Li, Inorg. Chem. Commun. 9 (2006) 205–207.
[26] Q. Su, Q. Wu, G. Li, X. Liu, Y. Mu, Polyhedron 26 (2007) 5053–5060.
[27] K.Y. Hwang, H. Kim, Y.S. Lee, M.H. Lee, Y. Do, Chem. Eur. J. 15 (2009) 6478–6487.
[28] V. Liuzzo, W. Oberhauser, A. Pucci, Inorg. Chem. Commun. 13 (2010) 686–688.
[29] T. Feng, H.M. Peng, Y.M. Yao, Y. Zhang, Q. Shen, Y.X. Cheng, Chin. Sci. Bull. 56 (2011) 1471–1475.
[30] G.G. Guilbault (Ed.), Practical Photoluminescence, second ed., Marcel Dekker, New York, 1990.
[31] A. Gilbert, J. Bagott, Essentials of Molecular Photochemistry, CRC Press, Boca Raton Inc., Florida, 1991.

[32] A.A. Abdel Aziz, Synth. React. Inorg. Met.-Org. Chem. 41 (2011) 384–393.
[33] A.I. Vogel, Text Book of Quantitative Chemical Analysis, fifth ed., Longmans, London, 1998.
[34] J. Olmsted, J. Phys. Chem. 83 (1979) 2581–2584.
[35] S. Basak, S. Sen, S. Banerjee, S. Mitra, G. Rosair, G.M.T. Rodriguez, Polyhedron 26 (2007) 5104–5112.
[36] M.J. Relezar, E.C.S. Chan, N.R. Kreig, Microbiology, fifth ed., McGraw Hill, New York, 1998.
[37] C.H. Collins, P.M. Lyne, Microbial Methods, University Park Press, Baltimore, 1970.
[38] J.A. Dean, Lange's Hand Book of Chemistry, fourth ed., McGraw-Hill, New York, 1992.
[39] S. Zolezzi, A. Decinti, E. Spodine, Polyhedron 18 (1999) 897–904.
[40] K. Ueno, A.E. Martel, J. Phys. Chem. 60 (1956) 1270–1275.
[41] P.E. Aranha, M.P. dos Santos, S. Romera, E.R. Dockal, Polyhedron 26 (2007) 1373–1382.
[42] J.E. Kovacic, Spectrochim. Acta A 23 (1967) 183–187.
[43] M.M. Omar, G.G. Mohamed, Spectrochim. Acta A 61 (2005) 929–936.
[44] L.J. Bellamy, The Infrared Spectra of Complex Molecules, third ed., Chapman and Hall, London, 1975.
[45] M. Tümer, N. Deligönül, A. Gölcü, E. Akgün, M. Dolaz, H. Demirelli, M. Dığrak, Trans. Met. Chem. 31 (2006) 1–12.
[46] M. Odabaşoğlu, F. Arslan, H. Ölmez, O. Büyükgüngör, Dyes Pigments 75 (2007) 507–515.
[47] H. Naeimi, J. Safari, A. Heidarnezhad, Dyes Pigments 73 (2007) 251–253.
[48] A. Majumder, G.M. Rosair, A. Mallick, N. Chattopadhyay, S. Mitra, Polyhedron 25 (2006) 1753–1762.
[49] M. Gullotti, A. Pasini, G.M. Zanderighi, G. Ciani, A. Sironi, J. Chem. Soc. Dalton Trans. (1981) 902–908.
[50] K. Singh, M.S. Barwa, P. Tyagi, Eur. J. Med. Chem. 41 (2006) 147–153.
[51] M. Tümer, D. Ekinci, F. Tümer, A. Bulut, Spectrochim. Acta A 67 (2007) 916–929.
[52] D. Pucci, I. Aiello, A. Bellusci, A. Crispini, M. Ghedini, M.L. Deda, Eur. J. Inorg. Chem. 28 (2009) 4274–4281.
[53] M. Vicente, R. Bastida, C. Lodeiro, A. Macías, A.J. Parola, L. Valencia, S.E. Spey, Inorg. Chem. 42 (2003) 6768–6779.
[54] H. Zengin, M. Dolaz, A. Gölcü, Anal. Chem. 5 (2009) 358–362.
[55] L.Z. Cai, W.T. Chen, M.S. Wang, G.C. Guo, J.S. Huang, Inorg. Chem. Commun. 7 (2004) 611–614.
[56] Y.D. Cao, Q.Y. Zheng, C.F. Chen, Z.T. Huang, Tetrahedron Lett. 44 (2003) 4751–4755.
[57] J.D. Ingle, S.R. Crouch, Spectrochemical Analysis, Prentice-Hall, Inc., New Jersey, 1988.
[58] S.M. Yue, H.B. Xu, J.F. Ma, Z.M. Su, Y.H. Kan, H.J. Zhang, Polyhedron 25 (2006) 635–644.
[59] Y.P. Tong, S.L. Zheng, X.M. Chen, J. Mol. Struct. 826 (2007) 104–112.
[60] R.C. Evans, P. Douglas, C.G. Winscom, Coor. Chem. Rev. 250 (2006) 2093–2126.
[61] S.K. Mandal, K. Nag, J. Chem. Soc. Dalton Trans. 11 (1983) 2429–2434.
[62] C.E. Overton, Studien uber die Narkose zugleich ein Beitrag zur allgemeinen Pharmakologie, Gustav Fischer, Jena, Switzerland, 1901.
[63] B.G. Tweedy, Phytopathalogy 55 (1964) 910–914.
[64] R. Tokuyama, Y. Takahashi, Y. Tomita, M. Tsubouchi, T. Yoshida, N. Iwasaki, N. Kado, E. Okezaki, O. Nagata, Chem. Pharm. Bull. 49 (2001) 353–360.